Supplement for manuscript

Effects of meteorology and emissions on urban air quality: a quantitative statistical approach to long-term records (1999–2016) in Seoul, South Korea

Jihoon Seo[1,2], Doo-Sun R. Park[3], Jin Young Kim[1], Daeok Youn[4], Yong Bin Lim[1], Yumi Kim[5]

[1]Green City Technology Institute, Korea Institute of Science and Technology, Seoul, 02792, South Korea
[2]School of Earth and Environmental Sciences, Seoul National University, Seoul 08826, South Korea
[3]Department of Earth Sciences, Chosun University, Gwangju 61452, South Korea
[4]Department of Earth Science Education, Chungbuk National University, Cheongju 28644, South Korea
[5]Division of Resource and Energy Assessment, Korea Environment Institute, Sejong 30147, South Korea
Correspondence to: Jin Young Kim (jykim@kist.re.kr), Daeok Youn (dyoun@chungbuk.ac.kr)

Contents: 1 table and 7 figures

Table S1. Degrees of freedom (*dof*) of each time series of short-term, baseline, and long-term components calculated based on Leith (1973).

dof	PM_{10}	SO_2	NO_2	CO	$O_{3\ 8h}$	T	T_{max}	P	RH	WS	SI
X_{ST}	1054	1084	1084	1084	1626	1084	1084	1084	1084	1626	1622
X_{BL}	45	45	55	35	50	46	47	47	60	36	58
X_{LT}	2	5	2	4	2	7	7	9	7	2	8
$X_{\mathrm{LT}}^{\mathrm{emis}}$	2	6	4	8	2						
$X_{\mathrm{LT}}^{\mathrm{met}}$	3	6	3	2	2						

Leith, C. E.: The standard error of time-average estimates of climatic means, J. Appl. Meteor., 12, 1066–1069, https://doi.org/10.1175/1520-0450(1973)012<1066:TSEOTA>2.0.CO;2, 1973.

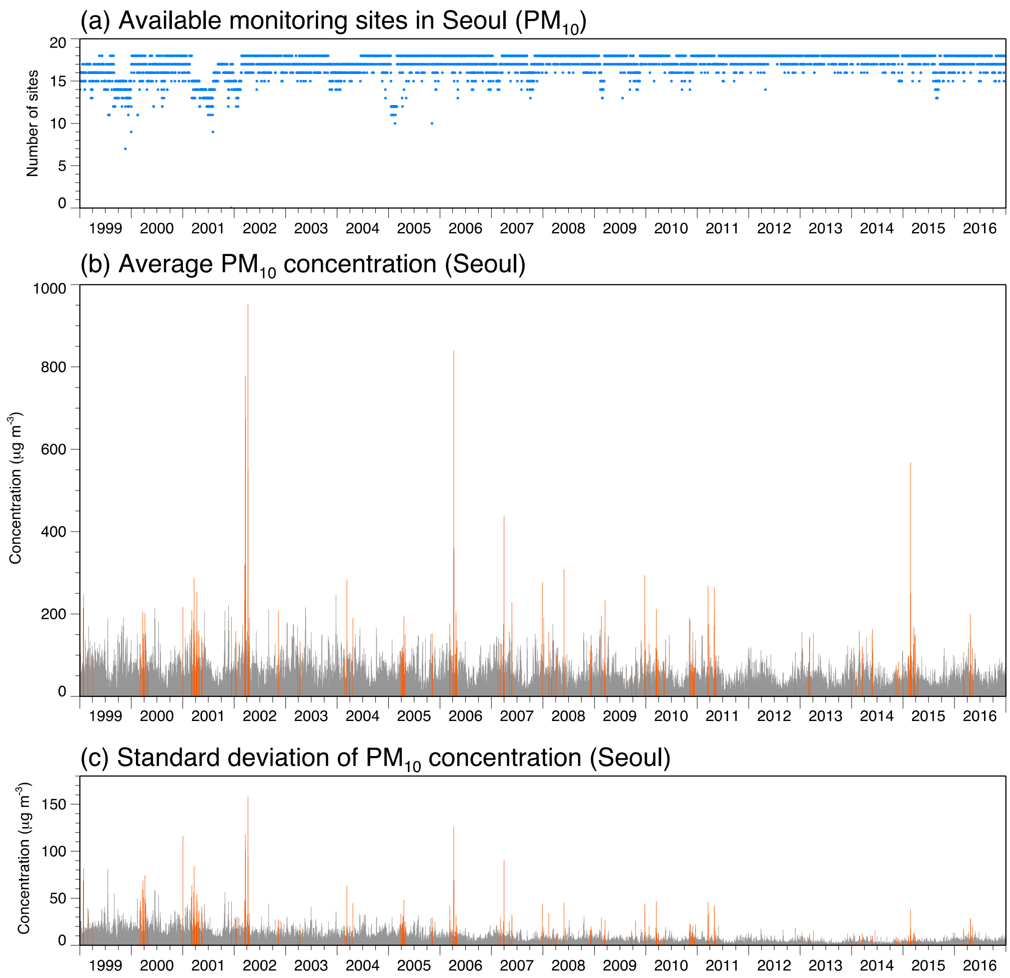

Figure S1. (a) Numbers of available air quality monitoring sites in Seoul, of which missing data are less than 10% of the total. (b) Average and (c) standard deviation of PM_{10} concentrations in Seoul. Asian dust events those were excluded from the PM_{10} analysis are marked with orange color.

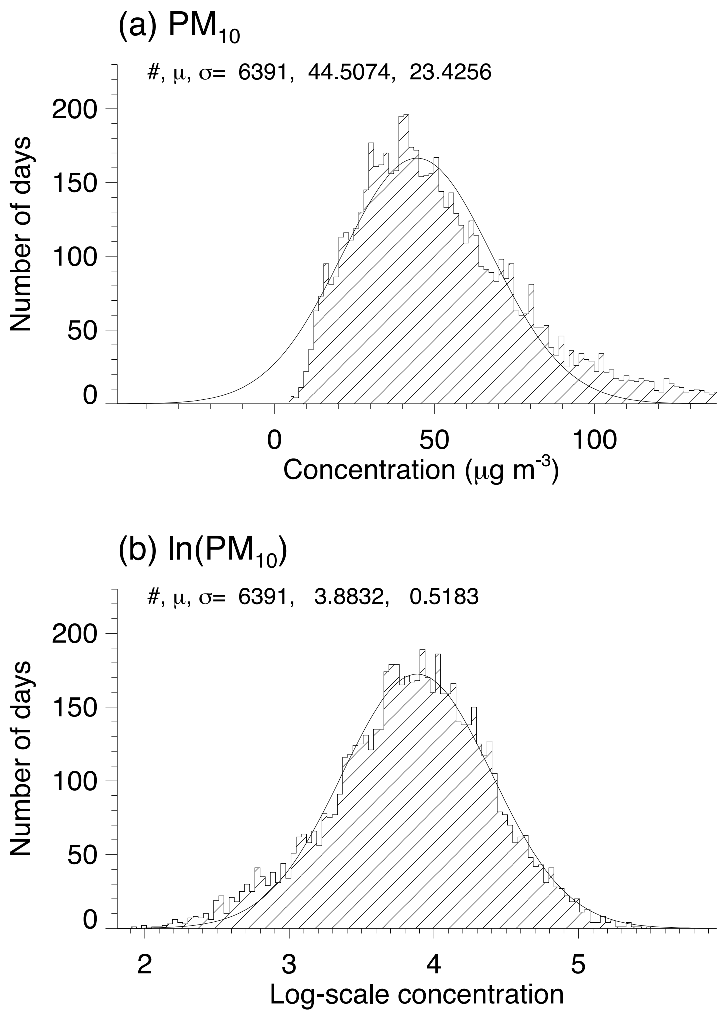

Figure S2. Number distribution of (a) daily average PM_{10} concentration and (b) log-transformed daily average PM_{10} concentration. The bell shaped curves show normal (Gaussian) distributions, and #, *μ*, and *σ* denote the total number of days, mean values, and standard deviation, respectively. Asian dust event days were excluded from the analysis.

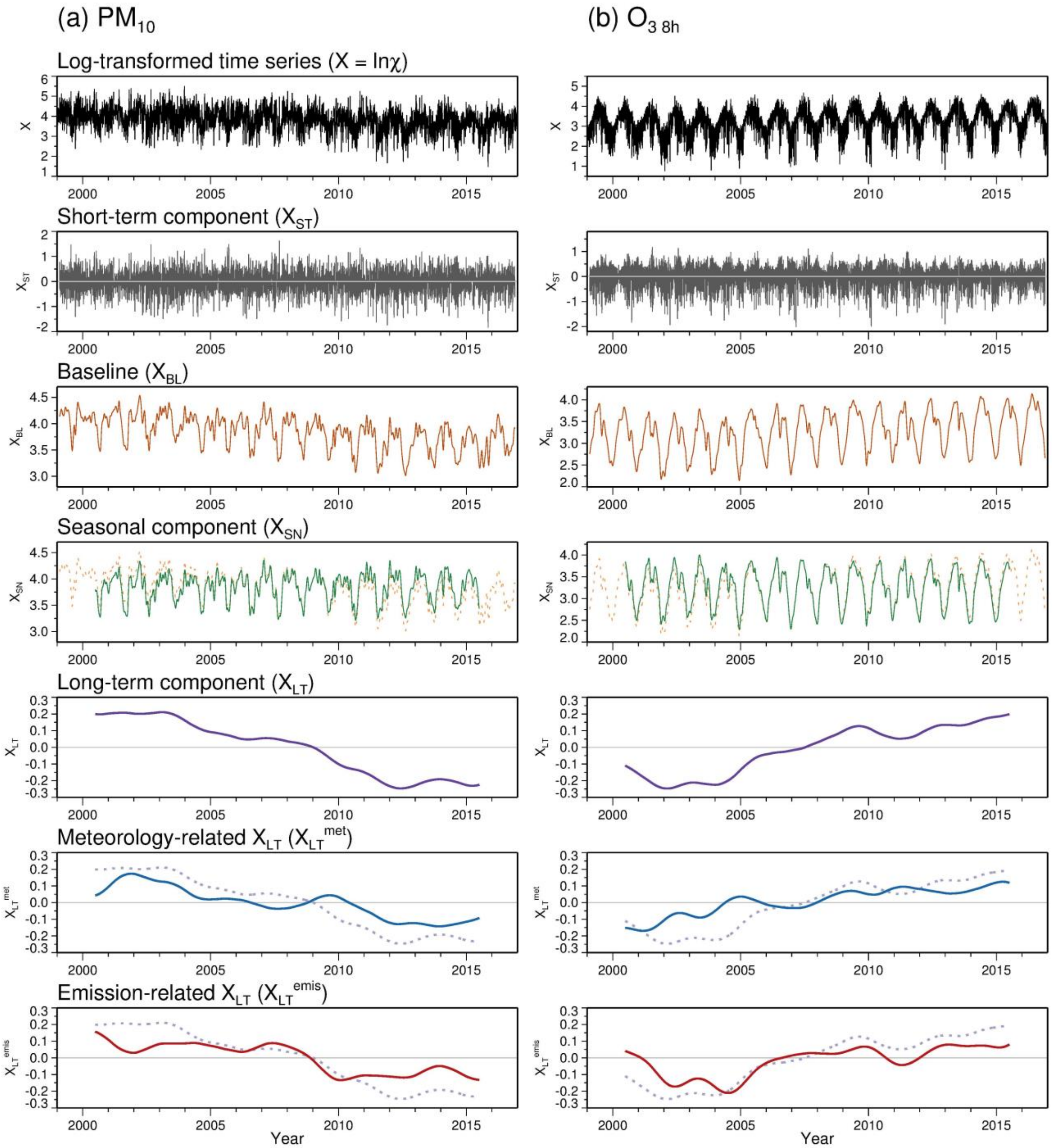

Figure S3. Decompositions of (a) PM_{10} and (b) $O_{3\ 8h}$ time series in Seoul for 1999–2016.

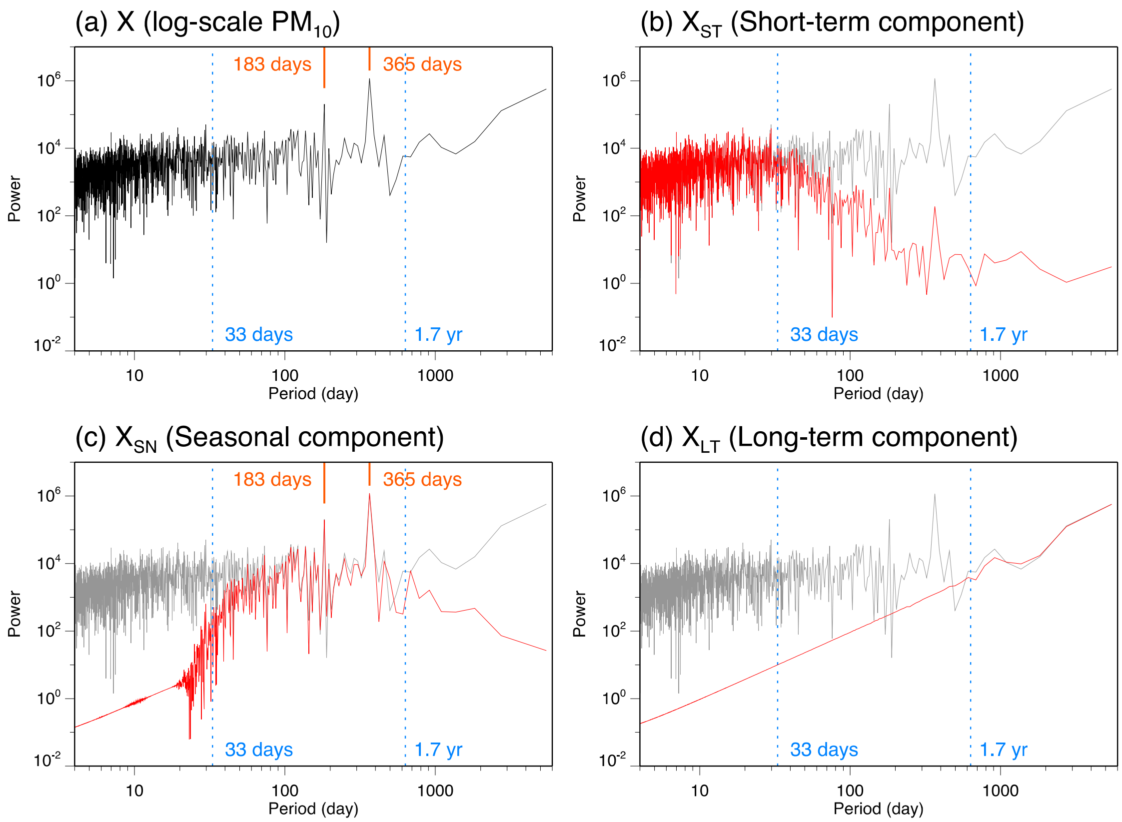

Figure S4. Power spectra of (a) log-transformed daily average PM_{10} concentration time series (a black line) and its (b) short-term, (c) seasonal, and (d) long-term components (red lines). Effective filter widths for $KZ_{(15,5)}$ filter (33 days) and $KZ_{(365,3)}$ filter (632 days) are marked with blue vertical dashed lines.

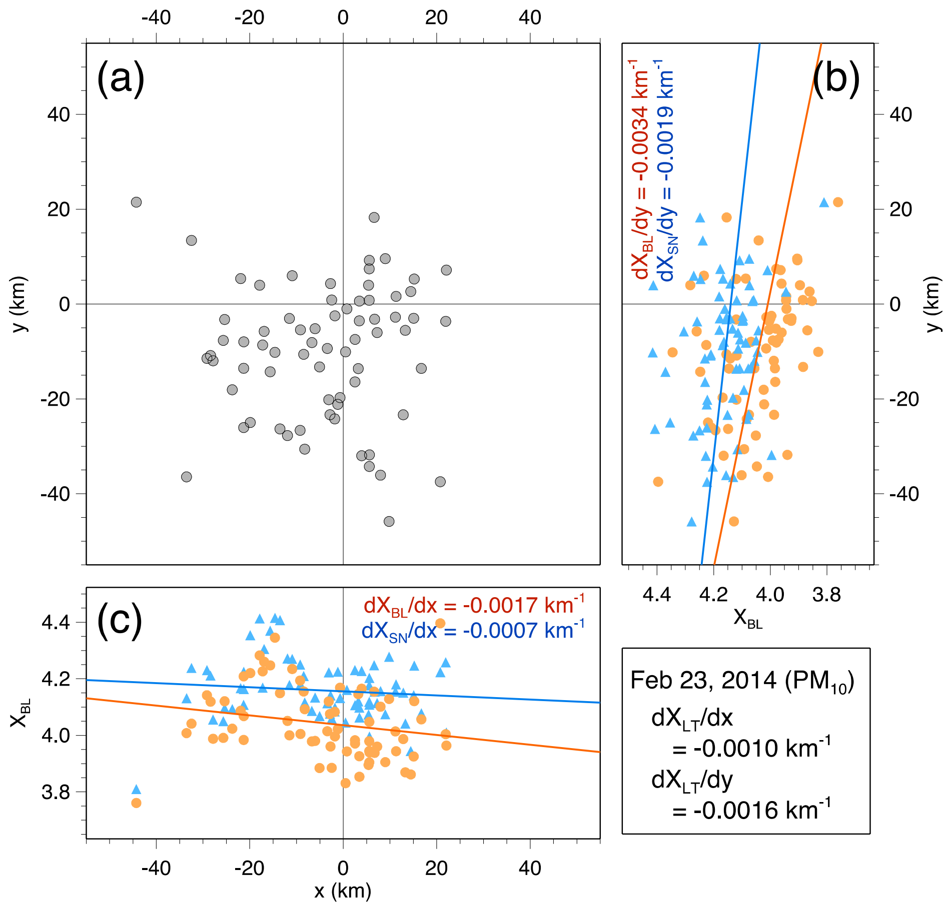

Figure S5. An example of obtaining horizontal gradient of long-term component (X_{LT}) of PM_{10} on 23 February 2014. (a) Locations of 70 air quality monitoring sites in Cartesian coordinates centered at the Seoul weather station (37.57°N, 126.97°E), of which data availability were more than 75% for the period of 1999–2016. (b) Meridional gradients of the baseline ($\frac{\partial X_{BL}}{\partial y}$) and seasonal component ($\frac{\partial X_{SN}}{\partial y}$) obtained by linear regressions. (c) Zonal gradients of the baseline ($\frac{\partial X_{BL}}{\partial x}$) and seasonal component ($\frac{\partial X_{SN}}{\partial x}$). Zonal and meridional gradient of the long-term component can be gained by subtracting the seasonal component gradients from the baseline gradients ($\frac{\partial X_{LT}}{\partial x} = \frac{\partial X_{BL}}{\partial x} - \frac{\partial X_{SN}}{\partial x}$, $\frac{\partial X_{LT}}{\partial y} = \frac{\partial X_{BL}}{\partial y} - \frac{\partial X_{SN}}{\partial y}$).

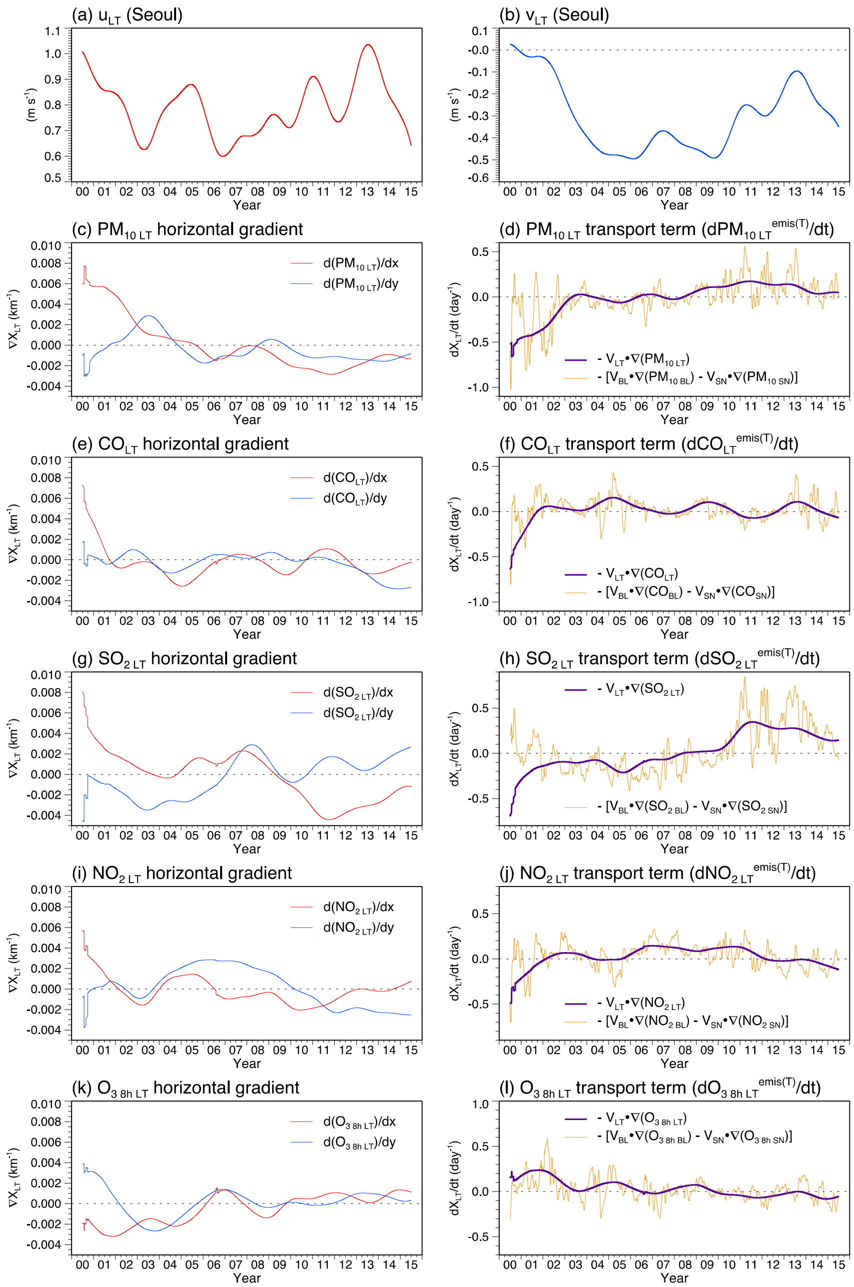

Figure S6. Long-term component of (a) zonal wind (u_{LT}) and (b) meridional wind (v_{LT}) at the Seoul weather station. Zonal gradient ($\partial X_{\mathrm{LT}}/\partial x$, red lines) and meridional gradients ($\partial X_{\mathrm{LT}}/\partial y$, blue lines) of the long-term components and transport term ($-\vec{V}_{\mathrm{LT}} \cdot \nabla X_{\mathrm{LT}}$, violet lines) by long-term components of horizontal winds ($\vec{V}_{\mathrm{LT}} = (u_{\mathrm{LT}}, v_{\mathrm{LT}})$) for (c–d) PM_{10}, (e–f) CO, (g–h) SO_2, (i–j) NO_2, (k–l) $O_{3\ 8h}$.

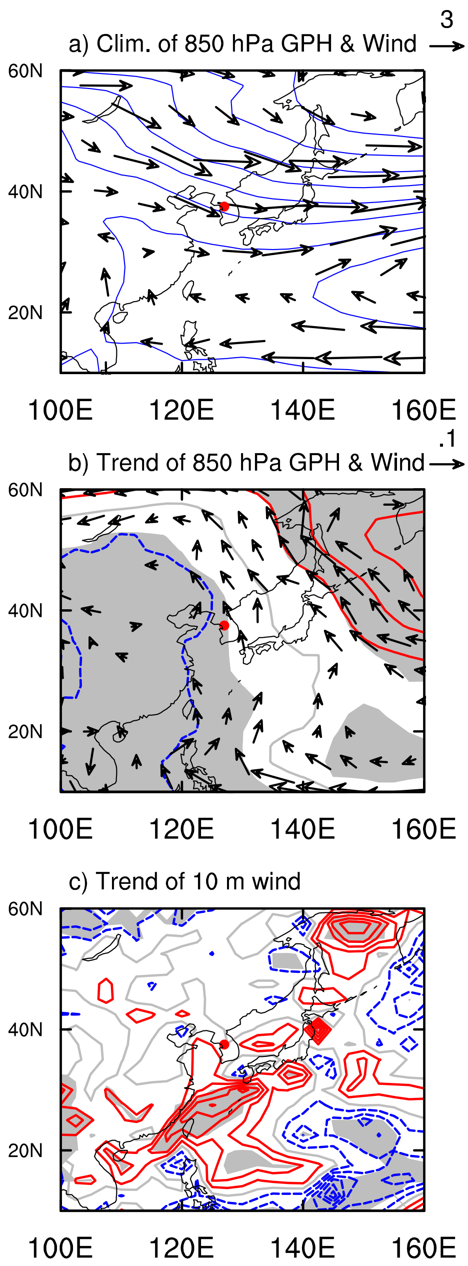

Figure S7. (a) Mean geopotential height (contours with interval of 20 gpm) and wind fields (arrows with reference scale of 3 m s^{-1}) at 850 hPa, and linear trends of (b) geopotential height (contours with interval of 0.5 gpm yr^{-1}) and wind (arrows with reference scale of 0.1 m s^{-1} yr^{-1}) at 850 hPa and (c) 10 m wind speed (contours with interval of 0.01 m s^{-1} yr^{-1}) for the period of 2000–2015. The trends statistically significant at 95% confidence level in (b) and (c) are represented as gray shaded areas and wind arrows. Seoul is marked by solid red circles.